Supplementary Data

1. Introduction

In line with the current goals of the NASA Mars exploration program (Hamilton *et al.*, 2015), we chose a field site having potential for past habitability (*i.e.*, a lacustrine environment) detectable using measurements from instruments at an outcrop that was analogous to future Mars landing sites. For this project we targeted the lacustrine Eocene Green River Formation in the Uinta Basin of northeastern Utah (Supplementary Fig. S1). The lacustrine deposits in this formation contain a variety of distinct biosignatures—microbial carbonates that could act as analogues for potential evidence of past life on Mars. Because its significance as a Mars analogue extends beyond this study, we include a comprehensive treatment of the geological history of the area here.

The Green River Formation, ranging from 300 to 2000 m of sedimentary strata, accumulated in and around ancient Lake Uinta. The open lacustrine environment of the Green River is represented by nearshore and offshore shales and mud-supported carbonates, including microbialites—stromatolites and thrombolites. Pisoids, ooids, oncoids, ostracods, and peloids are frequently associated with the microbial facies. Some of the best examples of all these characteristics are exposed in the upper Douglas Creek Member of the Green River Formation in and near the GeoHeuristic Operational Strategies (GHOST) field site called Gray Huts located in the southeastern part of the Uinta Basin (Supplementary Figs. S1 and S2). Green River outcrops at the Gray Huts field site and along nearby Evacuation Creek show meter-scale shallowing-up cycles composed of organic-rich shale through microbial carbonates (Supplementary Fig. S3).

2. Location

The Uinta Basin is located in the northern Colorado Plateau geological province between the Colorado state line and the Wasatch Plateau and thrust belt in north-central Utah. The basin is bounded on the north by the east-west-trending Uinta Mountains and on the south by the Book Cliffs (Supplementary Fig. S4). It is both a structural and topographic basin, dissected and drained by the Green River and its tributaries as part of the Colorado River system. The average elevation of the Uinta Basin is 1500 m (Hamblin, 2004); topographic relief at the study site is a maximum of 240 m. Like most areas in eastern Utah, the basin has a semiarid climate with low humidity, hot and dry summers, and cold winters. The average annual precipitation is 23.4 cm and vegetation consists of juniper, pinyon pine, and sage brush (dense in some areas). Topography is dominated by large canyons with steep slopes in soft bedrock and vertical cliffs composed of resistant rocks, both extending for several kilometers. Smaller narrow canyons are cut perpendicular to the major cliffs providing exceptional three-dimensional access to the rocks. The Gray Huts field site (39°48′17″N, 109°04′33″W) is within an unnamed canyon near the confluence of Evacuation and Missouri Creeks (Supplementary Figs. S1 and S2).

SUPPLEMENTARY FIG. S1. Location of the Gray Huts field site, eastern Uinta Basin, Utah.

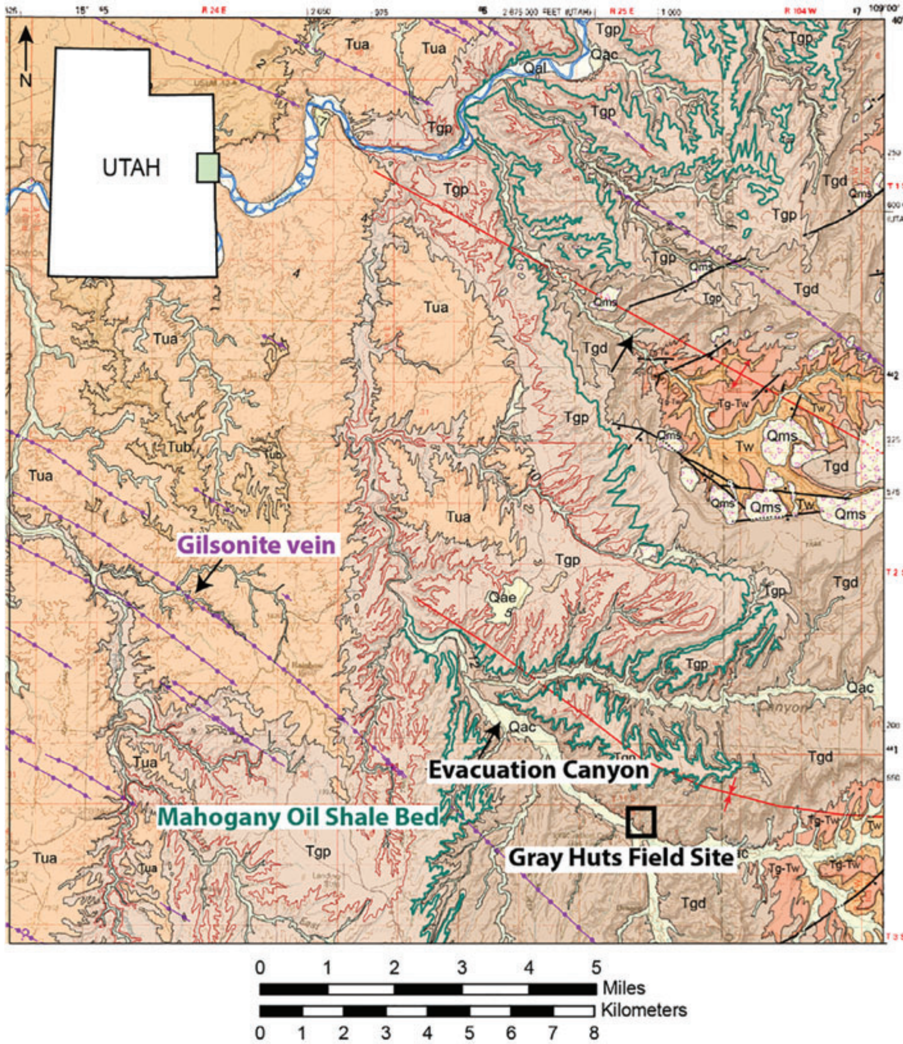

Stratigraphic Column

SYSTEM	SYMBOL	FORMATIONS	Thickness (meters) (not to scale)	NOTES
Quaternary	Q	Unconsolidated deposits	less than 50	Qal - stream alluvium, Qms - alluvial fan deposits, Qac - alluvium/colluvium, Qae - alluvium/eolian
Tertiary	Tub	Member B of Uinta Formation	30–225	Contains gilsonite deposits
	Tua	Member A of Uinta Formation	60–180	
	Tgp	Parachute Creek Member of Green River Formation	247–950	Tuffaceous bed B; Horse Bench Sandstone Bed; Mahogany oil shale zone
	Tgd	Douglas Creek Member of Green River Formation	45–520	Uinta Mountains continue to uplift and erode; creation of Lake Uinta as the Uinta Basin continues to subside; contains oil shale and oil reserves; Long Point Bed
	Tg-Tw	Green River-Wasatch Formations transition zone	60–220	Uinta Mountains continue to uplift and erode, locally exposing the Uinta Mountain Group; subsidence of Uinta Basin; gas reservoir in Uinta Basin
	Tw	Wasatch Formation	280–830	

SUPPLEMENTARY FIG. S2. Geological map of part of the eastern Uinta Basin showing outcrops of the Eocene Green River Formation, gilsonite veins, and the location of the Gray Huts field site. Stratigraphic column shows formations and members of the Cenozoic section, thickness, lithology, and major stratigraphic markers in the field site. Modified from Sprinkel (2009).

3. General Geological Setting

The Laramide orogeny, between latest Cretaceous and Eocene time, produced numerous basins and basement-cored uplifts in the Rocky Mountain states. The Uinta Basin is a major depositional and structural basin that subsided during the early Cenozoic along the southern flank of the Uinta Mountains. More than 3000 m of alluvial and lacustrine deposits filled the basin between the eroding Sevier highlands to the west and the rising Laramide-age Uinta Mountains,

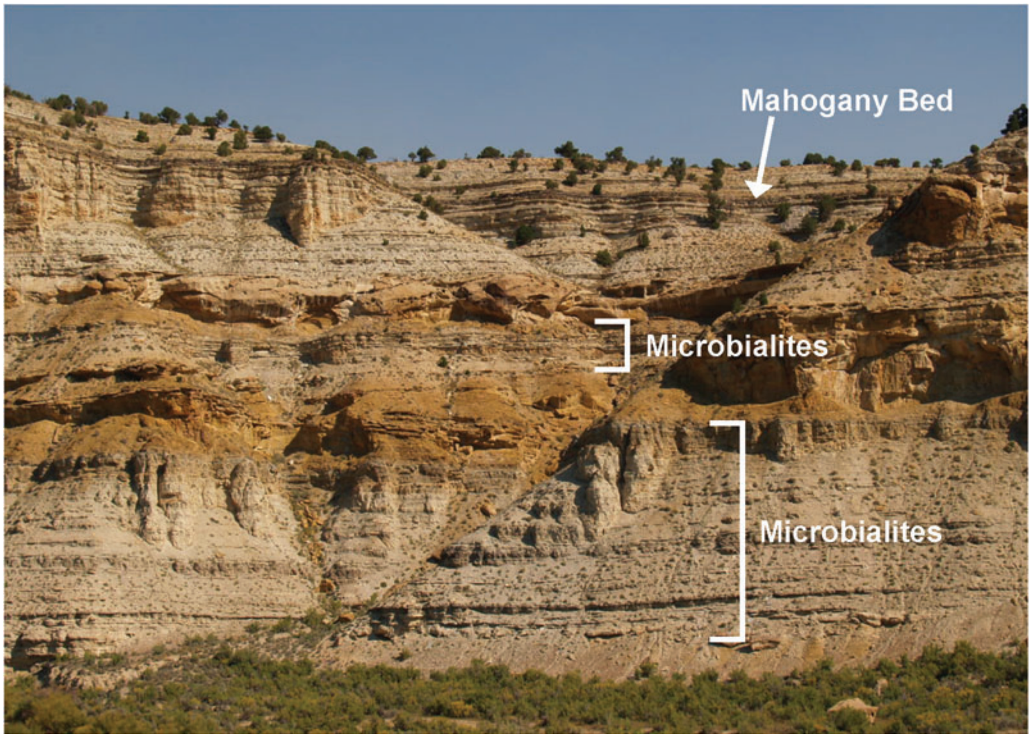

SUPPLEMENTARY FIG. S3. Typical outcrop of the lacustrine Eocene Green River Formation, Evacuation Creek area near the Gray Huts field site, eastern Uinta Basin, Utah. Note the meter-scale shallowing-up cycles composed of organic-rich shale, including the Mahogany oil shale bed, up to microbialite-bearing carbonate intervals.

Uncompahgre uplift, and San Rafael Swell to the north, east, and south, respectively (Hintze and Kowallis, 2009). Freshwater lakes developed between the eroding Sevier highlands to the west and the rising Laramide-age uplifts to the north, east, and south. During the Eocene, Lake Uinta formed in the Uinta Basin where alluvial, marginal lacustrine, and open lacustrine sediments accumulated in an intertonguing relationship. At times of high water level, Lake Uinta filled both the Uinta Basin and Colorado's Piceance Basin (Supplementary Fig. S5).

The Uinta Basin is asymmetrical to the north, paralleling the east-west-trending Uinta Mountains. The north flank dips 10–35° south into the basin and is bounded by a large north-dipping basement-involved thrust fault. The southern flank gently dips between 4° and 6° north-northwest from the Book Cliffs. Structures within the basin include small normal faults and fracture zones, large and small but subtle folds, and northwest-southeast-trending gilsonite (black solid hydrocarbon) veins that reflect the buried Laramide-age Uncompahgre uplift (Supplementary Figs. S2 and S4). Regional uplift of the Colorado Plateau occurred throughout the Cenozoic primarily due to the Laramide orogeny and isostatic rebound from erosion. This uplift changed the landscape from one of deposition to erosion (Lucchitta, 1979; Pederson *et al.*, 2002). The drainage pattern on the plateau was disrupted 5–6 million years ago (Ma) by major normal faults along the Basin and Range transition zone, resulting in erosion removing several thousand meters of Cretaceous and Tertiary sedimentary rocks and the relatively rapid incision of the Green River and its tributaries in the Uinta Basin (Lucchitta, 1989; Potochnik and Faulds, 1998).

4. Stratigraphy and Depositional History

4.1. Green River Formation

4.1.1. Stratigraphic overview. The Green River Formation consists of as much as 2000 m of sedimentary strata (Hintze and Kowallis, 2009; Sprinkel, 2009). The stratigraphy is complex, and for decades many different unit names and marker beds have appeared in the literature or have been used by industry (see Fouch, 1975, 1976; Ryder *et al.*, 1976; Fouch *et al.*, 1992; Morgan *et al.*, 2003, and the references pertaining to Green River nomenclature therein). Describing and explaining in detail Green River stratigraphy are beyond the scope of the Supplementary Data; instead, we provide a general summation in Fig. 6. The signature of each marker bed on wireline well logs is used to identify and correlate units in the subsurface throughout much of the basin. In brief, the Wasatch Formation grades upward into and intertongues with the Green River Formation in the Uinta Basin, forming the Green River–Wasatch Formation transition unit (Sprinkel, 2009). In general, the lower member of the Green River consists of the basal Uteland Butte member representing the first transgression of Lake Uinta (Fig. 6). After regression of the lake was a period of siliciclastic deposition represented by the Colton/Wasatch Tongue over which the Long Point transgression deposited the carbonate marker bed (Supplementary Fig. S6) and resulted in one lake in Utah and Colorado (Supplementary Fig. S5). The last major occurrence of mollusks is in these deposits, after which the lake turned saline and remained so until its end. The lower and middle members are separated by the carbonate marker bed. The middle member is called

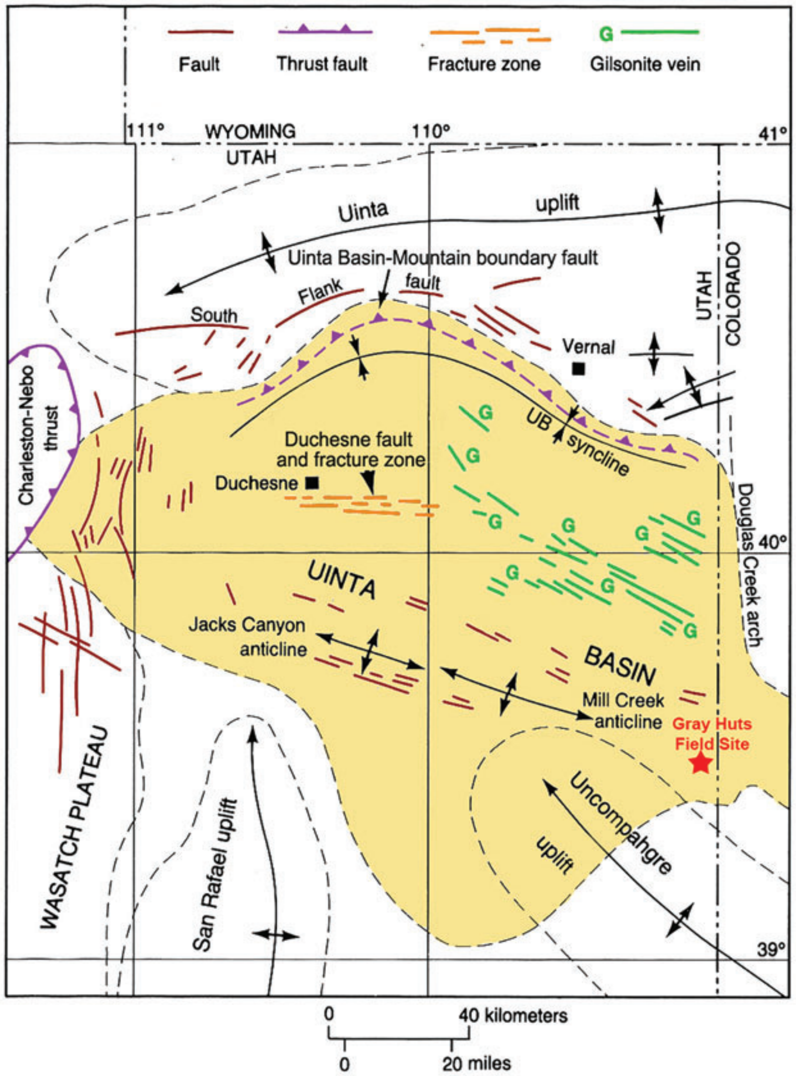

SUPPLEMENTARY FIG. S4. Schematic map of the major structural features, surface faults, and fracture zones in and around the Uinta Basin. Uinta Basin–Mountain boundary fault after Osmond (1986); other faults and gilsonite veins from Hintze (1997) and Hintze *et al.* (2000).

the Douglas Creek Member on most maps and publications and contains what is referred to as the ''delta facies'' and ''green shale facies'' in the western part of the basin (Supplementary Fig. S6); as mentioned earlier the facies examined by the rover GHOST test are within the upper Douglas Creek. The upper member, named the Parachute Creek Member, contains the famous Mahogany oil shale bed (zone) above the ''transitional facies'' (Supplementary Fig. S6). The Parachute Creek interfingers with the overlying Uinta Formation. The Douglas Creek and Parachute Creek Members are well exposed in the study area and contain abundant microbial carbonates.

4.1.2. Paleogeography and depositional environments. During late Paleocene and Eocene, the Uinta Basin and much of central and southern Utah was dominated by freshwater lakes and associated deltas, with periods of alluvial clastic deposition as the lakes eventually disappeared. The Green River Formation was deposited in the extensive shallow saline to freshwater Lake Uinta in the subsiding Uinta Basin (Supplementary Figs. S5 and S7). A generalized basin and regional scale depositional setting for Lake Uinta compares lake-level highstands, when carbonate deposition was widespread, with lowstands, when siliciclastic alluvial, fluvial, and eolian sediments were more common (Supplementary Fig. S7). The Green River contains three major depositional facies associated with Lake Uinta sedimentation: alluvial, marginal lacustrine, and open lacustrine (Supplementary Fig. S8) (Fouch, 1975). The Uteland Butte limestone records the first major transgression of Eocene Lake Uinta and thus it is relatively widespread in the basin. The marginal lacustrine facies consists of fluvial–deltaic, interdeltaic, and carbonate flat deposits (Supplementary Figs. S7 and S9), including microbialites. The position of these deposits changed as the lake shoreline shifted rapidly in response to sediment input and lake-level fluctuations (Supplementary Fig. S7).

The Uinta Mountains were the source for the sediments in the northern part of Lake Uinta, whereas sediments in the southern part of the lake were sourced from the much larger (but lower relief) Four Corners and areas to the southwest in California (Dickinson *et al.*, 1988; Blakey and Ranney, 2008). The open-lacustrine facies is represented by near-shore and deeper water offshore muds, including the famous

SUPPLEMENTARY FIG. S5. Eocene lake basins of the Rocky Mountain West. Lake Gosiute occupied the Green River and Washakie Basins in Wyoming, while Lake Uinta filled the Uinta and Piceance Basins in Utah and Colorado. Modified from Vanden Berg (2011).

Mahogany oil-shale zone, which represents Lake Uinta's highest water level (US Geological Survey Oil Shale Assessment Team, 2010; Tänavsuu-Milkeviciene and Sarg, 2012). Lake Uinta existed for ∼13 Ma and at its maximum extended into northwestern Colorado (Weiss *et al.*, 1990). During the late middle to early late Eocene, Lake Uinta began to shrink in response to tectonic changes and stream capture, creating several phases of hypersalinity (Vanden Berg and Birgenheier, 2017).

4.1.3. Douglas Creek Member. The siliciclastic-dominated Douglas Creek Member ranges in thickness from 45 to 520 m (Supplementary Figs. S2 and S6), and consists of light- to medium-gray, light- to medium-brown, yellow, and light-gray siltstone, sandstone, shale, chert, and limestone (Sprinkel, 2009). The Douglas Creek is dominated by shallowing-upward sequences of mudstones, siltstones, and sandstones, often gradually transitioning to well-developed microbial carbonates at the uppermost part of the cycles. The carbonates are commonly topped by erosional flooding surfaces and sometimes preserve transgressive lag material. Sandstone is generally fine grained, moderately to well sorted, thin to thick bedded, discontinuous, and lenticular, mainly in channel bodies, and contains cross-stratified to planar beds, ripple marks, and scours (Gualtieri, 1988; Weiss *et al.*, 1990; Sprinkel, 2009). Limestone contains boundstone, rudstone, grainstone, packstone, wackestone, and mudstone carbonate fabrics. Constituent carbonate grains include ooids, pisoids, peloids, oncoids, coated grains, and skeletal material, especially ostracods and/or storm-generated carbonate rip-up clasts. Microbial carbonates include both stromatolites and thrombolites that often developed on a grainstone or rip-up substrates (Supplementary Fig. S9) (Chidsey *et al.*, 2015). The Douglas Creek also contains some thin bluish-gray (weathered) to dark brown oil shale. The member forms large vertical cliffs, ledges, and steep slopes.

4.1.4. Parachute Creek Member. The Parachute Creek Member contains large-scale carbonate-dominated and siliciclastic sequences (Supplementary Fig. S6). It ranges in thickness from 250 to 950 m (Supplementary Fig. S2) and consists of moderately resistant, light- to medium-gray, light- to medium-brown, and yellow shale, marlstone and limestone, siltstone, and sandstone (Sprinkel, 2009). The Parachute Creek records carbonate-dominated shallowing-upward sequences, with carbonate mudstones transitioning to dolomitic microbial carbonates topped by an erosional flooding surface (Chidsey *et al.*, 2015). Carbonates are similar to those in the underlying Douglas Creek Member and are dominated by oolites and microbialites. Both marlstone and shale can be dark brown and organic rich, including several oil shale beds, the most significant being the Mahogany oil-shale zone (Supplementary Figs. S2, S3, and S10). Siliciclastic intervals are very fine to medium grained and thin to thick bedded, containing cross-laminations and ripple marks (Gualtieri, 1988). The Parachute Creek also contains dated tuff beds and an interval of nahcolite nodules near the top (''Birds Nest'' aquifer zone) (Supplementary Figs. S6 and S11). The Parachute Creek forms steep slopes, cliffs, and ledges.

4.2. *Quaternary deposits*

Relatively thin unconsolidated gravel, sand, silt, and clay are found in a variety of settings—the products of weathering, running water, wind, and mass wasting as the Uinta Basin are currently in a state of regional erosion. Quaternary deposits are found throughout the area (Supplementary Fig. S2) and although they may appear insignificant in comparison with bedrock formations, it is important to recognize their presence and describe characteristics that may be analogous to those found on Mars.

The beginning of the Quaternary within the Colorado Plateau was characterized by the development of stream and river drainages across the lower elevations of the landscape. Preserved deposits are mostly unconsolidated and vary in thickness depending on their depositional environment. The most common Quaternary (Holocene to late Pleistocene) materials are thin (<10 m) stream alluvial deposits composed of poorly to well-sorted sand, silt, and pebbles and alluvial mud. However, colluvial, eolian, alluvial fan, and alluvial gravel deposits are also found in the area (Sprinkel, 2009). Within the field site, unmapped stream alluvial deposits occur in active ephemeral stream channels in canyons, and colluvium covers most of the steep slopes.

5. Evacuation Creek Area and the Gray Huts Field Site

5.1. *General geological description*

Extensive outcrops of the Parachute Creek and the upper part of the Douglas Creek Members of the Green River

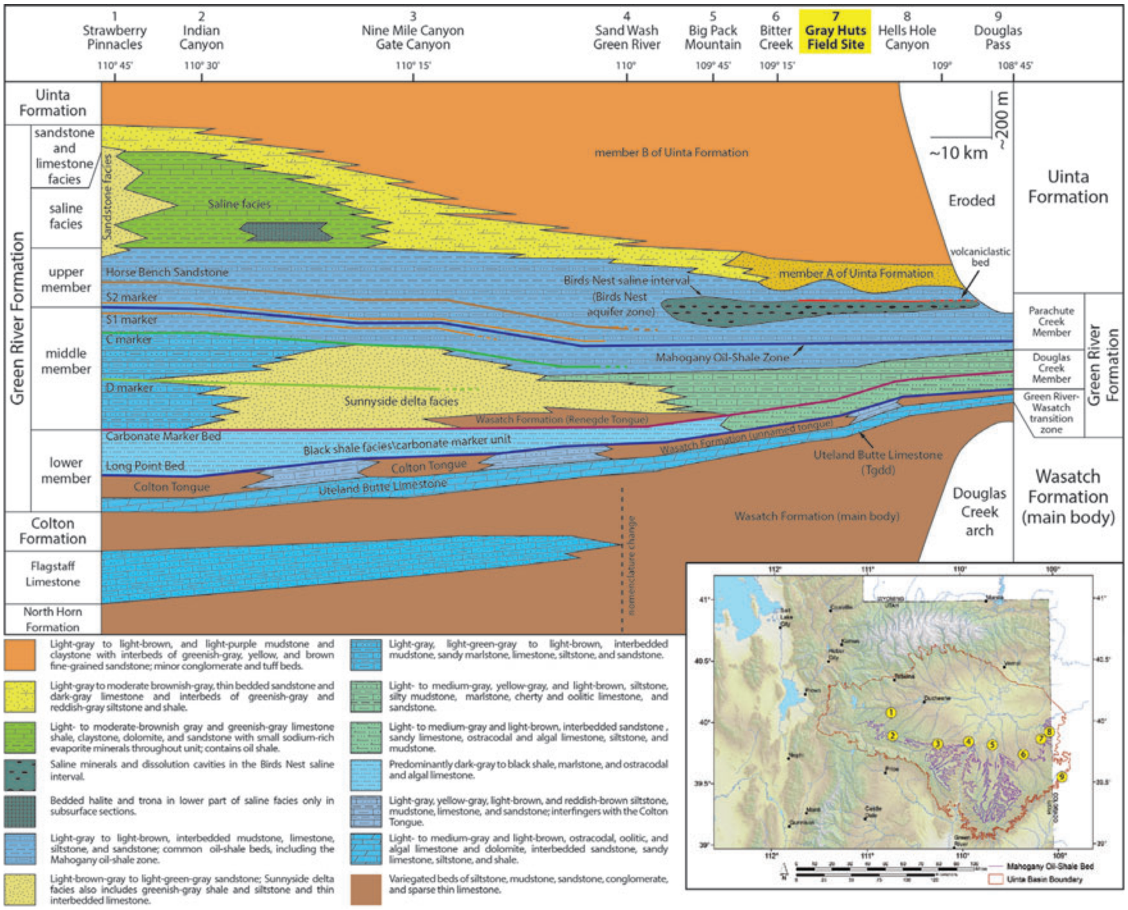

SUPPLEMENTARY FIG. S6. General stratigraphy and major marker beds of the Green River Formation in the Uinta Basin. After Sprinkel (in preparation), modified from Töro and Pratt (2015) using Cashion (1967), Johnson *et al.* (1988, 2010), Fouch *et al.* (1994), Morgan *et al.* (2003), Smith *et al.* (2008), Tänavsuu-Milkeviciene and Sarg (2012), and Vanden Berg *et al.* (2013).

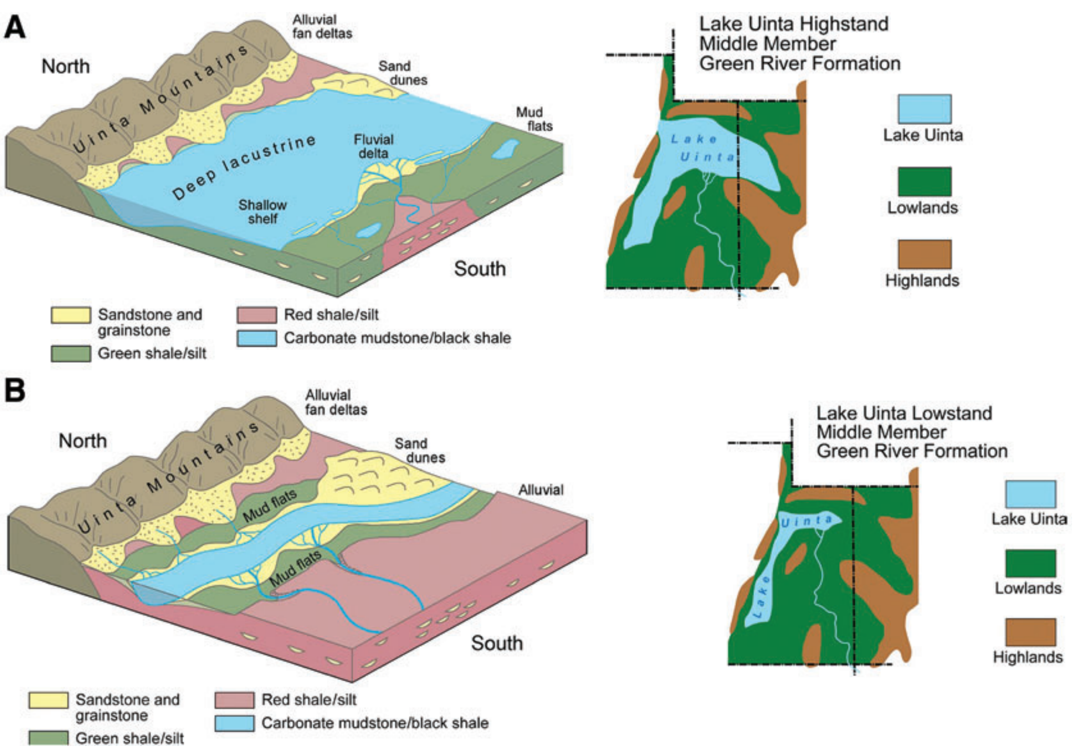

SUPPLEMENTARY FIG. S7. Generalized depositional setting for Lake Uinta (55–45 million years [Ma]): **(A)** high lake levels and **(B)** low lake levels. From Morgan *et al.* (2003).

SUPPLEMENTARY FIG. S8. Eocene paleogeography of the Uinta Basin during deposition of the Douglas Creek Member (middle member) of the Green River Formation in open-lake and marginal lacustrine environments. Modified from Fouch (1975) and Fouch *et al.* (1992).

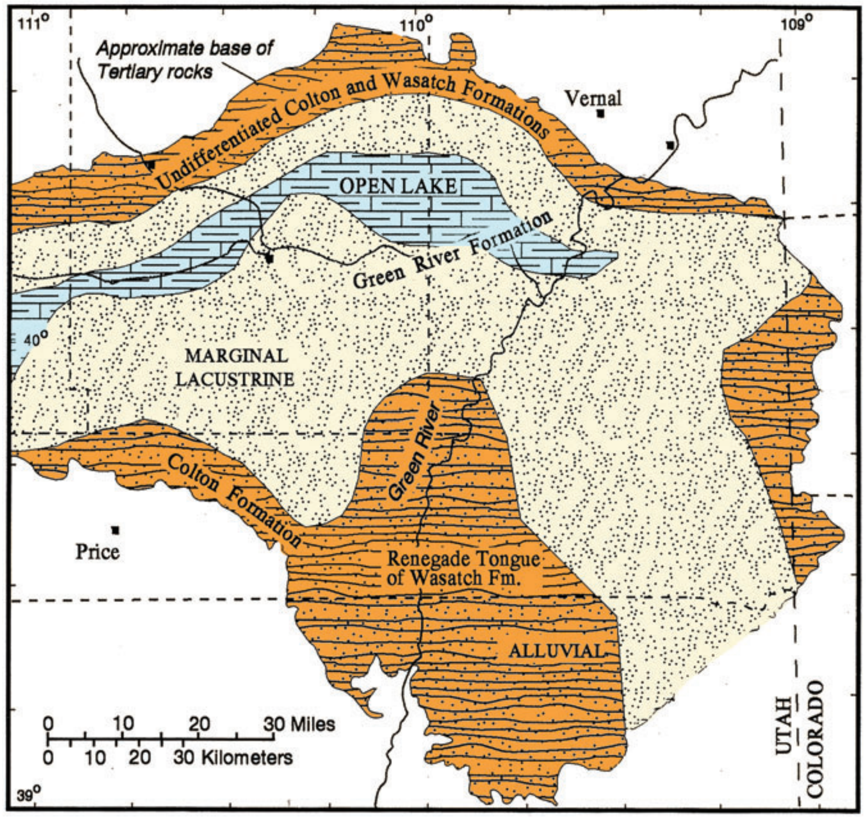

SUPPLEMENTARY FIG. S9. A typical Green River microbialite interval and associated facies, Hells Hole area, eastern Uinta Basin. The light tan interval near the base is composed of pisoids and oncoids (as a grainstone/rudstone). The tan beds beneath the hammer are stromatolitic, whereas thrombolites dominate the area to the right of the hammer.

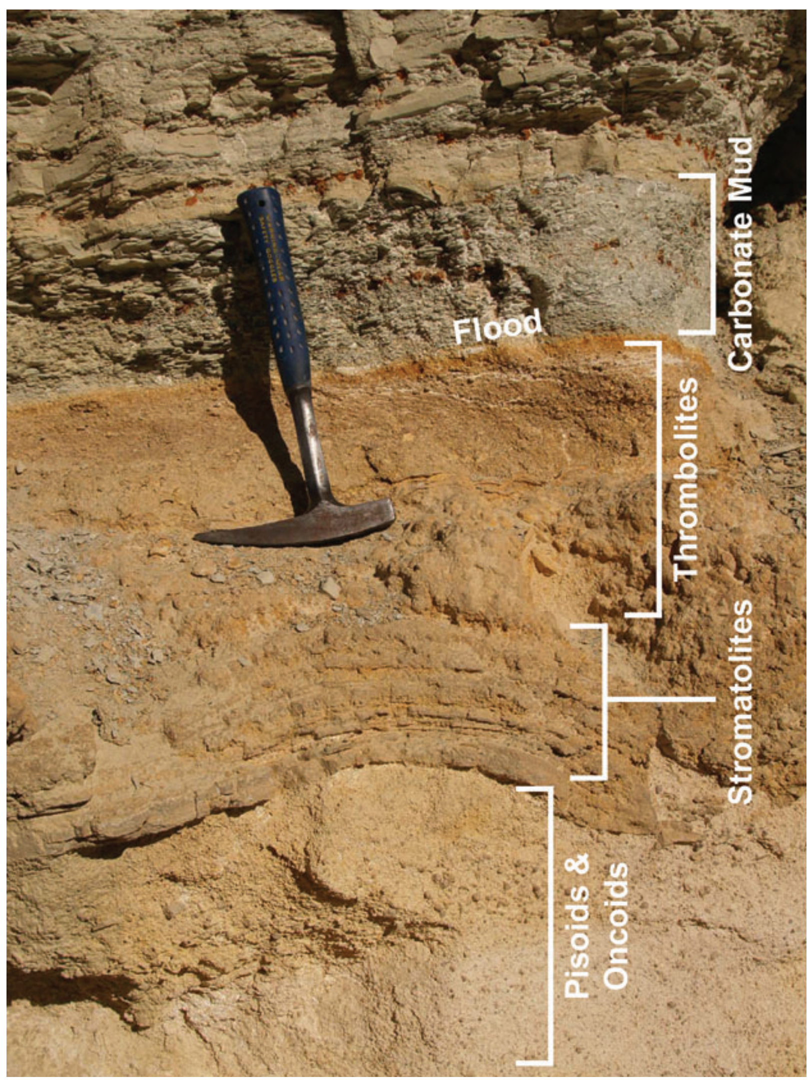

SUPPLEMENTARY FIG. S10. Mahogany oil shale zone, Parachute Creek Member, Evacuation Creek area, eastern Uinta Basin; view to the west.

SUPPLEMENTARY FIG. S11. The ''Birds Nest'' aquifer zone with dissolved nahcolite nodules in the upper Parachute Creek Member, representing hypersaline conditions during the waning stage of Lake Uinta, Evacuation Creek, eastern Uinta Basin; view to the north.

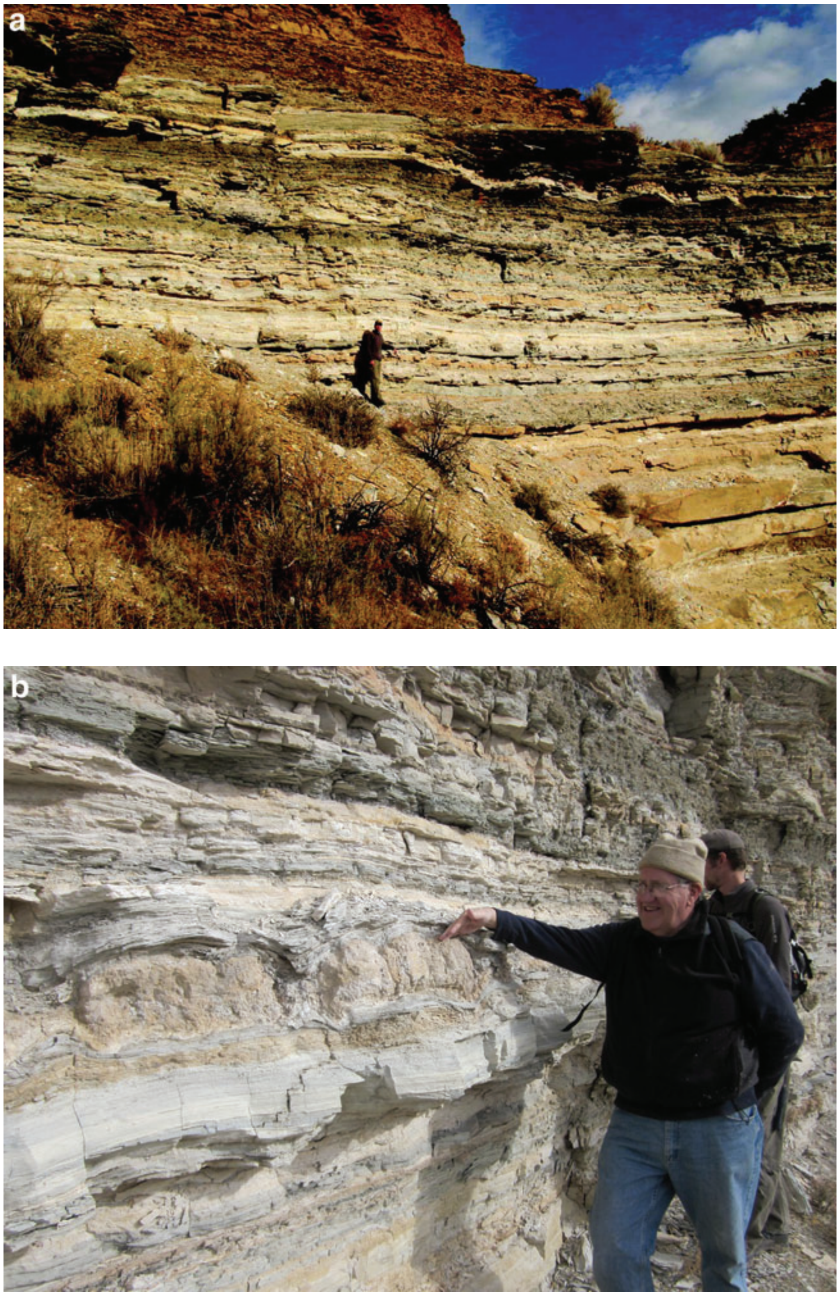

SUPPLEMENTARY FIG. 12. (Continued).

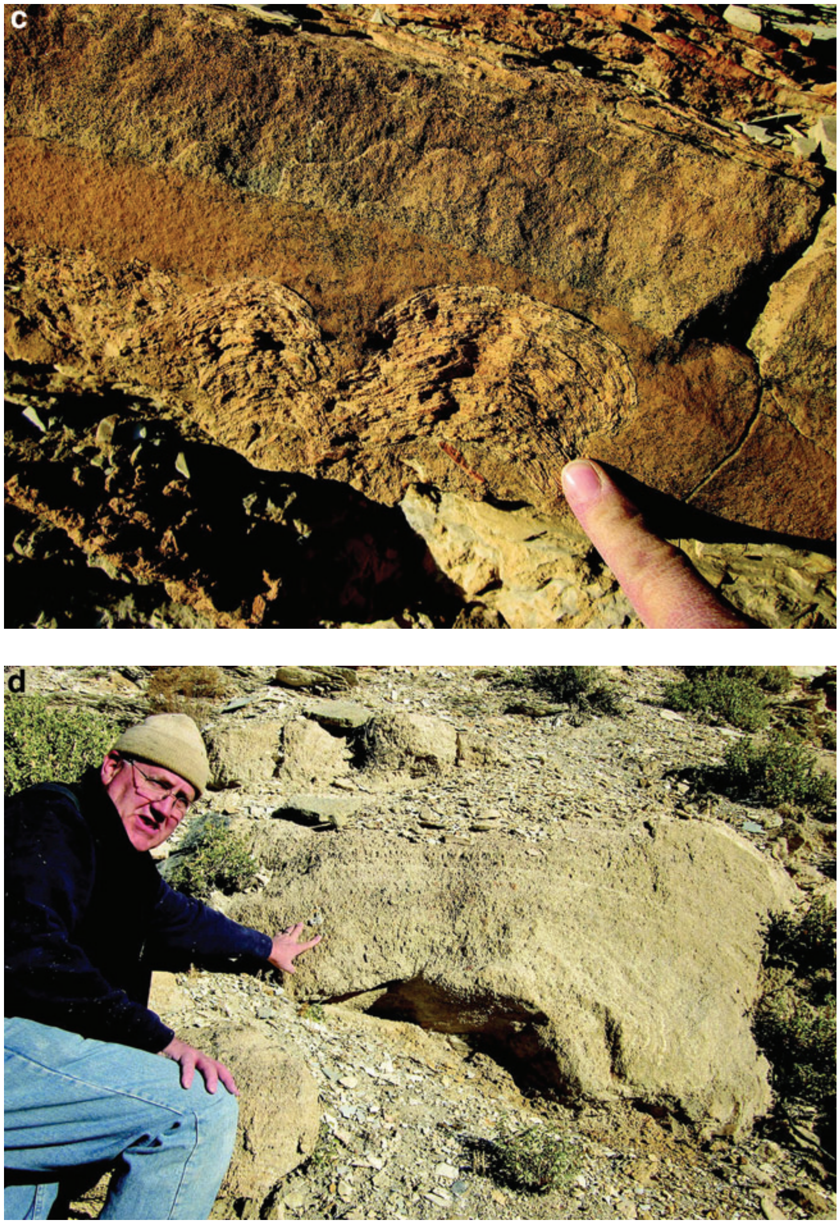

SUPPLEMENTARY FIG. 12. (Continued).

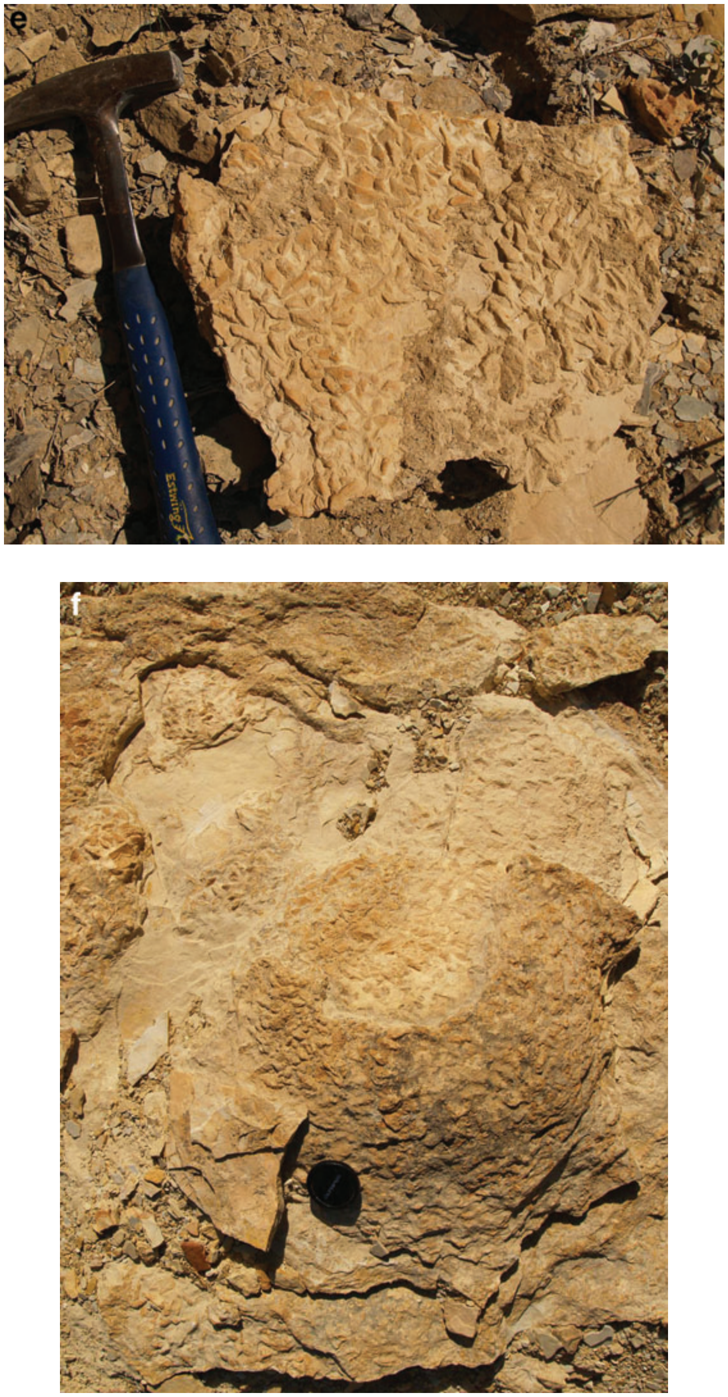

SUPPLEMENTARY FIG. S12. Parachute Creek Member of the Green River Formation in the Evacuation Creek area. **(a)** View of part of the Flash Flood section in which microbialites (yellowish) and associated carbonate facies are present. **(b)** Outcrop view of representative thin continuous stromatolite beds in the light brown colors (below hand). **(c)** Small domal stromatolite heads (adjacent to the finger). **(d)** A meter-scale thrombolite head. Note the steep margin of this domal structure. **(e)** Photo of evaporite crystal casts. **(f)** Plan view of stromatolite with crystal molds located on the dome.

Formation in the Evacuation Creek area contain excellent examples of lacustrine facies including microbial carbonates. Several outcrop sites have been studied in the Evacuation Creek area by Chidsey *et al.* (2015), Rosenberg *et al.* (2015), and Rosencrans (2015) to (1) determine the distribution and lateral continuity of microbialites and related carbonate facies, (2) place the microbialites and other carbonate facies into the depositional context of the lake history, and (3) examine the sedimentology and stratigraphy of deltaic distal mouth bar complexes. The characteristics, geometry, distribution, and bounding surfaces of the lacustrine facies and associated microbialites could be analogous to what may be found on Mars.

The Parachute Creek Member along Evacuation Creek contains dolomitic and limy mudstones with well-displayed porous microbialites including stromatolites and thrombolites. Grainstones composed of ooids, coated grains, pisolites, and peloids often overlie and underlie the microbialites.

In general, shale and its organic content increase up section indicating deeper water depths of Lake Uinta. This is best reflected by the excellent exposures of the classic organic-rich shale of the Mahogany bed near the top of the section (Supplementary Fig. S1). Microbialites and associated facies are most heavily concentrated in the lower part of the Parachute Creek and the Douglas Creek Members (Supplementary Figs. S2 and S12a). In addition, multiple packages of fluvial–deltaic sandstones punctuate the lacustrine sediments, which are composed of limestone, claystone, and siltstone. Rosenberg *et al.* (2015) and Rosencrans (2015) identified several examples of very fine-grained sandstone beds that interrupt microbial sequences and represent deposition in distributary and distal mouth bar complexes sourced by rivers flowing from the southeast to the northwest. In some parts of the section, shale beds overlie thin small microbial heads and represent deepening events or parasequence boundaries.

Among the microbialites well displayed in the Evacuation Creek outcrops are stromatolites and thrombolites. Stromatolites may be bedded and continuous laterally for tens of meters (Supplementary Fig. S12b), whereas others have small domal heads (Supplementary Fig. S12c) grading upward into branching digitate forms. Thrombolites are also laterally extensive, especially near the base of the section, and domal with synoptic relief (Supplementary Fig. S12d). Thrombolites contain large open pores (vugs) resulting from microbial construction.

The relatively shallow water lake margin, carbonate flat environment of Lake Uinta was the ideal site in terms of water chemistry, temperature, and depth for microbial growth along with oolite, oncolite, and peloid formation, as observed in the Evacuation Creek outcrops. The salinity of Lake Uinta must have been at times fairly high (15–16%) to sustain microbial growth and carbonate grain formation. In addition, large casts of crystals suggesting evidence of exposure (Supplementary Fig. S12e, f) can be traced over significant lateral distances. Some examples wrap around or appear to encrust small microbial heads.

A shallow ramp, as evidenced by Parachute Creek and other Green River Formation deposits, created susceptibility to rapid widespread shoreline changes, which were not conducive to thick accumulations of microbialite buildups. Instead, deposits are dominated by 1 to 2 m shallowing-upward sequences having only several tens of centimeters of porous microbialite formation, which are interbedded with profundal shales.

Carbonate muds and ooids often provided the adequate substrate for microbial mat formation, but in other cases microbialites grew on accumulations of carbonate rip-up material. Currents along the lake margins would supply nutrients for these microbial communities, as well as keep the area relatively free of suffocating mud (Osmond, 2000).

SUPPLEMENTARY FIG. S13. The Gray Huts field site; view to the southwest toward Evacuation Creek.

5.2. Gray Huts

Outcrops at Gray Huts field site (Supplementary Fig. S13) are composed of upper Douglas Creek Member deposits of the Green River Formation and were studied in detail by Rosenberg *et al.* (2015), Rosencrans (2015), and Cupertino *et al.* (2018); the results are summarized here. Near the base of the exposed section not far into the canyon are fine- to medium-grained sandstone units interpreted as littoral distributary channel and proximal fluvial mouth bar deposits; organic-poor laminated siltstone and claystone represent distal mouth bar facies (Rosenberg *et al.*, 2015). The site displays three transgressive microbialite-bearing carbonate intervals (Cupertino *et al.*, 2018). Each interval is capped by siliciclastics interpreted as prograding deltas.

The lowest microbial carbonate interval is the most laterally continuous. Microbial thrombolites, 1 m thick, can be traced from Gray Huts along Evacuation Creek. The vertical succession consists of coarsening-upward grainstones containing ostracods with rip-up clasts, ooids, peloids, and oncolites, overlain by microbialites. All are dominated by dolomite (80%). The microbialites contain beds of layered (undulatory to pseudocolumnar), minicolumnar, and closely spaced domical stromatolites. The lowest interval was deposited on a littoral high-energy carbonate ramp with little siliciclastic input (Rosenberg *et al.*, 2015; Cupertino *et al.*, 2018).

The middle interval has lateral facies variations ranging from well-developed large microbialites (central area, Supplementary Fig. S14a) to smaller bioherms and ostracodal–ooidal grainstones to the northwest to organic-rich mudstones to the southeast. The interval is dominated by dolomite (70% with ≤10% quartz grains). The interval begins with a debris layer that is the substrate for the overlying microbialites; other microbial-bearing zones overlay organic-poor carbonate mudstone. The microbialites are composed of domical stromatolites (≤80 cm) (Supplementary Fig. S14b, c) followed by 50–70 cm of shrubby branching, minicolumnar stromatolites, then 10–30 cm thick columnar stromatolites, and culminates with 0–50 cm of microbial boundstone interpreted as a sublittoral low-energy carbonate ramp (Rosenberg *et al.*, 2015; Cupertino *et al.*, 2018). The middle interval was superimposed on the lowstand delta on the lower unit that ended the first cycle. The higher siliciclastic content of the middle interval and the δ^{18}O signal indicate that the delta was active during transgression (Cupertino *et al.*, 2018).

SUPPLEMENTARY FIG. S14. Middle interval, Gray Huts field site. **(a)** Panorama, with person for scale, **(b)** top view of stromatolite heads, **(c)** cross-sectional view of large digitate finely laminated columns.

The upper interval is composed of undulatory, pseudo-columnar to columnar stromatolites, and microbial boundstones that were deposited on top of paleohighs created by the older larger microbialites. Ostracodal–oolitic grainstones and organic-rich mudstones were deposited in surrounding paleolows. The lithology is dominated by dolomite (83%) with some calcite and ankerite. The upper interval shows no fluvial influence and was deposited in slightly deeper water as indicated by a heavier $\delta^{18}O$ signal and represents a sublittoral low-energy carbonate ramp (Rosenberg *et al.*, 2015; Cupertino *et al.*, 2018).

Supplementary References

Blakey, R.C. and Ranney, W. (2008) *Ancient Landscapes of the Colorado Plateau*. Grand Canyon Association, U.S. Geological Survey, Restin, VA, 156 p.

Cashion, W.B. (1967) Geology and fuel resources of the Green River Formation, southeastern Uinta Basin, Utah and Colorado [Paper No. 548]. US Geological Survey Professional Paper, 48 p.

Chidsey, T.C., Jr., Vanden Berg, M.D., and Eby, D.E. (2015) Petrography and characterization of microbial carbonates and associated facies from modern Great Salt Lake and Uinta Basin's Eocene Green River Formation in Utah, USA. In *Microbial Carbonates in Space and Time—Implications for Global Exploration and Production*, Geological Society Special Publication No. 418, edited by D.W.J. Bosence, K.A. Gibbon, D.P. Le Heron, W.A. Morgan, T. Pritchard, and B.A. Vining, The Geological Society, London, pp 261–286.

Cupertino, D., Vanden Berg, M., Awramik, S., Buchheim, C., Frantz, C., and Chidsey, T.C., Jr. (2018) Microbialite investigations of the Douglas Creek Member of the Green River Formation (Eocene), Evacuation Creek area, Uinta Basin, Utah, USA [abstract]. In American Association of Petroleum Geologists Annual Convention Abstracts Volume, nonpagenated.

Dickinson, W.R., Klute, M.A., Hayes, M.J., Janecke, S.U., Lundin, E.R., McKittrick, M.A., and Olivares, M.D. (1988) Paleogeographic and paleotectonic setting of Laramide sedimentary basins in the central Rocky Mountain region. *Geol Soc Am Bull* 100:1023–1039.

Fouch, T.D. (1975) Lithofacies and related hydrocarbon accumulations in Tertiary strata of the western and central Uinta Basin, Utah. In *Symposium on Deep Drilling Frontiers in the Central Rocky Mountains*, edited by D.W. Bolyard, Rocky Mountain Association of Geologists Guidebook, Rocky Mountain Association of Geology, Denver, CO, pp 163–173.

Fouch, T.D. (1976) *Revision of the Lower Part of the Tertiary System in the Central and Western Uinta Basin, Utah*. US Geological Survey Bulletin 1405-C, U.S. Geological Survey, Restin, VA, 7 p.

Fouch, T.D., Nuccio, V.F., Osmond, J.C., MacMillan, L., Cashion, W.B., and Wandrey, C.J. (1992) Oil and gas in uppermost Cretaceous and Tertiary rock, Uinta Basin, Utah. In *Hydrocarbon and Mineral Resources of the Uinta Basin, Utah and Colorado*, Utah Geological Association Publication No. 20, edited by T.D. Fouch, V.F. Nuccio, and T.C. Chidsey, Jr., Utah Geological Association, Salt Lake City, UT, pp 9–47.

Fouch, T.D., Nuccio, V.F., Anders, D.E., Rice, D.D., Pitman, J.K., and Mast, R.F. (1994) Green River (!) petroleum system, Uinta Basin, Utah, USA [Memoir 60]. In *The Petroleum System—from Source to Trap*, edited by L.B. Magoon and W.G. Dow, American Association of Petroleum Geologists, Tulsa, OK, pp 399–421.

Gualtieri, J.L. (1988) Geologic map of the Westwater $30' \times 60'$ quadrangle, Grand and Uintah Counties, Utah, and Garfield and Mesa Counties, Colorado. US Geological Survey Map I-1765, scale 1:100,000. U.S. Geological Survey, Restin, VA.

Hamblin, W.K. (2004) *Beyond the Visible Landscape—Aerial Panoramas of Utah's Geology*. Brigham Young University, Provo, Utah, 300 p.

Hamilton, V.E., Hoehler, T., Eigenbrode, J., Rafkin, S., Withers, P., Ruff, S., Yingst, R.A., Lim, D., Whitley, R., Beaty, D.W., Diniega, S., Hays, L., and Zurek, R. (2015) *Mars Scientific Goals, Objectives, Investigations, and Priorities: Mars Exploration Program Analysis Group (MEPAG) White Paper*, 74 p. Available online at mepag.jpl.nasa.gov/reports/MEPAG%20Goals_Document_2015_v18_FINAL.docx Last accessed January 16, 2020.

Hintze, L.F. (1997) Geological highway map of Utah. Geology Studies Special Publication No. 3, Brigham Young University, Provo, UT, scale 1:1,000,000.

Hintze, L.F. and Kowallis, B.J. (2009) Geologic history of Utah. Brigham Young University Geology Studies Special Publication No. 9, Brigham Young University, Provo, UT, 225 p.

Hintze, L.F., Willis, G.C., Laes, D.Y.M., Sprinkel, D.A., and Brown, K.D. (2000) Digital geologic map of Utah: Utah Geological Survey Map 179DM, scale 1:500,000. Utah Geological Survey, Salt Lake City, UT.

Johnson, R.C., Nichols, D.J., and Hanley, J.H. (1988) Stratigraphic sections of lower Tertiary strata and charts showing palynomorphs and mollusk assemblages, Douglas Creek arch area, Colorado and Utah. US Geological Survey Miscellaneous Field Studies MF-1997, 2 plates, scale 1:125,000. U.S. Geological Survey, Restin, VA.

Johnson, R.C., Mercier, T.J., Brownfield, M.E., and Self, J.G. (2010) Assessment of in-place oil shale resources in the Green River Formation, Uinta Basin, Utah and Colorado. US Geological Survey Digital Data Series DDS-69-BB, chapter 1, U.S. Geological Survey, Restin, VA, 153 pp.

Lucchitta, I. (1979) Late Cenozoic uplift of the southwestern Colorado Plateau and adjacent Colorado River region. *Tectonophysics* 61:63–95.

Lucchitta, I. (1989) History of the Grand Canyon and of the Colorado River in Arizona. In *Geologic Evolution of Arizona*, edited by J.P. Jenney and S.J. Reynolds, Arizona Geological Society Digest 17, Arizona Geological Survey, Phoenix, AZ, pp 701–715.

Morgan, C.D., Chidsey, T.C., Jr., McClure, K.P., Bereskin, S.R., and Deo, M.D. (2003) Reservoir characterization of the lower Green River Formation, southwest Uinta Basin, Utah. Utah Geological Survey Open-File Report 411, CD-ROM, 28 plates, Geological Society of America, Boulder, CO, 216 p.

Osmond, J.C. (1986) Petroleum geology of the Uinta Mountains—White River uplift, Colorado and Utah. In *New Interpretations of Northwest Colorado Geology*, edited by D.S. Stone, Rocky Mountain Association of Geologists Guidebook, Geological Society of America, Boulder, CO, pp 213–221.

Osmond, J.C. (2000) West Willow Creek field—first productive lacustrine stromatolite mound in the Eocene Green River Formation, Uinta Basin, Utah. *Mount Geol* 37:157–170.

Pederson, J., Karlstrom, K., Sharp, W., and McIntosh, W. (2002) Differential incision of the Grand Canyon related to

Quaternary faulting—constraints from U-series and Ar/Ar dating. *Geology* 30:739–742.

Potochnik, A.R. and Faulds, J.E. (1998) A tale of two rivers—tertiary structural inversion and drainage reversal across the southern boundary of the Colorado Plateau. In *Geologic Excursions in Northern and Central Arizona*, edited by E.M. Duebendorfer, Field Trip Guidebook for Geological Society of America Rocky Mountain Section Meeting, U.S. Geological Survey, Restin, VA, pp 149–173.

Rosenberg, M.J., Birgenheier, L.P., and Vanden Berg, M.D. (2015) Facies, stratigraphic architecture, and lake evolution of the oil shale bearing Green River Formation, eastern Uinta Basin, Utah. In *Stratigraphy and Paleolimnology of the Green River Formation, Western USA*, edited by M.E. Smith and A.R. Carroll, Syntheses in Limnology, vol. 1, Springer, American Association of Petroleum Geologists, Tulsa, OK, pp 211–249.

Rosencrans, E.M. (2015) Stratigraphic architecture of deltaic mouth bar deposits during early Eocene climatic optimum, Green River Formation, Uinta Basin, Utah. M.S. thesis, University of Utah, Salt Lake City, 148 p.

Ryder, R.T., Fouch, T.D., and Elison, J.H. (1976) Early tertiary sedimentation in the western Uinta Basin, Utah. *Geol Soc Am Bull* 87:496–512.

Smith, M.E., Carroll, A.R., and Singer, B.S. (2008) Synoptic reconstruction of a major ancient lake system—Eocene Green River Formation, western United States. *Geol Soc Am Bull* 120:54–84.

Sprinkel, D.A. (2009) Interim geologic map of the seep ridge 30′×60′ quadrangle, Uintah, Duchesne, and Carbon Counties, Utah, and Garfield and Rio Blanco Counties, Colorado. Utah Geological Survey Open-File Report 549, scale 1:100,000. Utah Geological Survey, Salt Lake City, UT.

Tänavsuu-Milkeviciene, K. and Sarg, F.J. (2012) Evolution of an organic-rich lake basin—stratigraphy, climate and tectonics—Piceance Creek basin, Eocene Green River Formation. *Sedimentology* 59:1735–1768.

Töro, B. and Pratt, B.R. (2015) Characteristics and implications of sedimentary deformation features in the Green River Formation (Eocene) in Utah and Colorado. In *Geology of Utah's Uinta Basin and Uinta Mountains*, Utah Geological Association Publication No. 44, edited by M.D. Vanden Berg, R. Ressetar, and L.P. Birgenheier, Utah Geological Survey, Salt Lake City, UT, pp 371–422.

US Geological Survey Oil Shale Assessment Team. (2010) Oil shale resources of the Uinta Basin, Utah and Colorado. US Geological Survey Digital Data Series DDS–69–BB, 7 chapters, CD. U.S. Geological Survey, Restin, VA.

Vanden Berg, M.D. (2011) Exploring Utah's other great lake. Utah Geological Survey, Survey Notes 43, Utah Geological Survey, Salt Lake City, UT, pp 1–2.

Vanden Berg, M.D. and Birgenheier, L.P. (2017) An examination of the hypersaline phases of Eocene Lake Uinta, upper Green River Formation, Uinta Basin, Utah. *J Paleolimnol* 58:353–371.

Vanden Berg, M.D., Lehle, D.R., Carney, S.M., and Morgan, C.D. (2013) Geological characterization of the Birds Nest aquifer, Uinta Basin, Utah—assessment of the aquifer's potential as a saline water disposal zone. Utah Geological Survey Special Study 147, Utah Geological Survey, Salt Lake City, UT, p 53.

Weiss, M.P., Witkind, I.J., and Cashion, W.B. (1990) Geologic map of the Price 30′×60′ quadrangle, Carbon, Duchesne, Uintah, Utah, and Wasatch Counties, Utah. US Geological Survey Miscellaneous Investigations Series Map I-1981, scale 1:100,000. U.S. Geological Survey, Restin, VA.

Supplementary Table S1. Estimated Sol Cost for All Activities by the Linear Team

Linear traverse sol path

Sol type	*Sol No.*	*Activity*
Drive/remote	1	Approach Station A Acquire 3 tier (ground to sky) 180° mosaic pointed ∼N Acquire single column vertical mosaic, 11 images
Drive/remote	2	Bump to Station A_a using images from the 180° mosaic Acquire 3×2 workspace mosaic Acquire 11 image vertical mosaic up from the workspace Acquire under-rover image Acquire clast survey (single image, starboard side of the rover)
Remote	3	Selected two spots for reflectance spectroscopy analysis—one on unit 2 and one on unit 3
Drive	4	Drive away from Station A_a toward Station B using images from Sol 1 180° mosaic Acquire new drive direction mosaic
Drive	5	Drive into mouth of canyon using Sol 4 drive direction mosaic Acquire new drive direction mosaic
Drive/remote	6	Drive to Station B Acquire 2 tier 270° mosaic from SSW to SSE
Drive/remote	7	Bump to Station B_a to investigate crinkly layer on top of unit 3 Acquire workspace mosaic Acquire one remote high resolution (millimeter scale) image of layer of interest
Remote	8	Acquire reflectance spectroscopy off clean portion of layer of interest
Drive/remote	9	Back up toward Station B, drive to Station B_b using Sol 6 mosaic Acquire 3×2 workspace mosaic

(*continued*)

Supplementary Table S1. (Continued)

Linear traverse sol path		
Sol type	*Sol No.*	*Activity*
Drive	10	Did not follow up on anything in the 3×2 workspace mosaic Back up from Station B_b to drive path and drive to end of mesh in Sol 6 mosaic Acquire drive direction mosaic along low road pathway
Drive	11	Drive along low road pathway to end of mesh Acquire drive direction mosaic that includes Station C
Drive/remote	12	Drive to Station C Acquire 3 tier 360° mosaic
Drive/remote	13	Drive to Station C_a Acquire mosaic along the pale tan horizon
Remote	14	Target upper and lower portions of the horizon with reflectance spectroscopy
Drive/remote	15	Bump closer to Station C_a Acquire 3×2 workspace mosaic
Contact	16	Select spot for sampling on layer with wavy laminations to plan drill placement Acquire close-approach submillimeter imaging (before dust removal and before drill loading test) Remove dust from the drill spot Acquire close-approach submillimeter images after dust removal Conduct preload test Acquire images after the drill loading test Acquire detailed elemental data from the drill spot
Contact	17	Using preload data, plan, and execute full drill activity (Station C_b) Acquire postdrill submillimeter images
Contact/remote	18	Deliver drill sample to XRD instrument During the day, collect any desired remote documentation of drill hole/tailings Acquire millimeter-scale remote imaging of drill hole for future reflectance spectroscopy targeting First high-resolution data integration of sample
Contact/remote	19	Acquire reflectance spectroscopy data from drill hole interior Complete any further daytime remote documentation of the drill hole/tailings At night, submillimeter imaging of drill hole interior and tailings Acquire detailed elemental data from the drill tailings
Drive/remote	20	Complete drill hole/tailings observations Back up to low road path from Station C_a, drive to Station C_b using Sol 12 360° mosaic Acquire 3×2 workspace mosaic
Remote	21	Acquire reflectance spectroscopy data from lower (C_{b1}) and lower (C_{b2}) portions of domed structure Conduct second mineralogical analysis of Station C_a sample
Drive/remote	22	Bump to drillable portion of Station C_b workspace (C_{b2} layer) Acquire workspace mosaic
Contact	23	Select postsieve dump site and drill target Acquire close-approach submillimeter imaging (before dust removal) Remove dust from the drill spot Acquire close-approach submillimeter images after dust removal Dump postsieve (Station C_a) sample Acquire context image of postsieve dump site Acquire detailed elemental data from the drill target
Contact	24	Acquire close-approach submillimeter imaging of postsieve dump pile Acquire close-approach submillimeter imaging before drill loading test Conduct drill loading test Acquire close-approach submillimeter imaging after the drill loading test Acquire detailed elemental data from the postsieve dump pile
Contact	25	Using preload data, plan and execute full drill activity (Station C_b) Acquire postdrill submillimeter images
Contact/remote	26	Deliver drill sample to XRD instrument During the day, collect any desired remote documentation of drill hole/tailings Acquire millimeter-scale remote imaging of drill hole for future reflectance spectroscopy targeting First high-resolution data integration of sample
Contact/remote	27	Acquire reflectance spectroscopy data from drill hole interior Complete any further daytime remote documentation of the drill hole/tailings

(*continued*)

Supplementary Table S1. (Continued)

Linear traverse sol path		
Sol type	*Sol No.*	*Activity*
		At night, submillimeter imaging of drill hole interior and tailings
		Acquire detailed elemental data from the drill tailings
Contact/drive/ remote	28	Complete drill hole/tailings observations
		Bump to horizon above C_{b2}
		Acquire 3×2 workspace mosaic
Remote	29	Acquire reflectance spectroscopy of horizon (C_{b3})
		Conduct second mineralogical analysis of Station C_b sample
Drive	30	Back up from C_b to low road path, drive along path to end of mesh from Sol 12 360° mosaic
		Acquire drive direction mosaic along low road pathway
Drive	31	Drive along low road pathway to end of mesh
		Acquire drive direction mosaic along low road pathway
Drive	32	Drive along low road pathway to end of mesh
		Acquire drive direction mosaic along low road pathway
Drive/remote	33	Drive to Station D
		Acquire 3 tier 360° mosaic, upper and midlevel tiers
		Acquire two mosaics along stream bed
Drive/remote	34	Bump to float rock in stream bed (Station D_a)
		Acquire workspace mosaic including rock
		Acquire vertical mosaic looking for traversable path up to layers of interest above Station D, both at context and high resolutions
Contact/remote	35	Acquire close-approach mosaic tracing layers laterally across the rock
		Acquire reflectance spectroscopy from rock
Contact	36	Select postsieve dump site and drill target (just for mineralogy, not for caching)
		Acquire close-approach submillimeter imaging of the drill target (before dust removal)
		Remove dust from the drill target
		Acquire close-approach submillimeter images of the drill target after dust removal
		Dump postsieve (Station C_b) sample
		Acquire context image of postsieve dump site
		Acquire detailed elemental data from the postsieve dump pile
Contact	37	Acquire close-approach submillimeter images of postsieve dump pile
		Acquire close-approach submillimeter imaging before drill loading test
		Conduct drill loading test
		Acquire close-approach submillimeter imaging after the drill loading test
		Acquire detailed elemental data from the postsieve dump pile
Contact	38	Using preload data, plan and execute full drill activity (Station D_a)
		Acquire postdrill close-approach submillimeter images
Contact/remote	39	Deliver drill sample to XRD instrument
		During the day, collect any desired remote documentation of drill hole/tailings
		Acquire millimeter-scale remote imaging of drill hole for future borehole observations
		Conduct first mineralogical analysis of Station D_a sample
Contact/remote	40	Acquire reflectance spectroscopy data from drill hole interior
		Complete any further daytime remote documentation of the drill hole/tailings
		At night, close-approach imaging of drill hole interior and tailings
		Acquire detailed elemental data from the drill tailings
Contact/drive/ remote	41	Complete drill hole/tailings observations
		Drive to first Station D workspace (D_b) using Sol 33 and 34 mosaics
		Acquire 3×2 workspace mosaic
		Conduct second mineralogical analysis of Station D_a sample
Contact/remote	42	Acquire reflectance spectroscopy data from workspace target
		Acquire close-approach submillimeter image from workspace target
		Acquire drive direction mosaic up slope toward next workspace of interest
Drive/remote	43	Drive to second Station D workspace (Station D_c)
		Acquire 3×2 workspace mosaic
Contact/remote	44	Acquire reflectance spectroscopy data from workspace target
		Acquire close-approach submillimeter image from workspace target
Contact	45	Select postsieve dump site and drill target

(*continued*)

Supplementary Table S1. (Continued)

Linear traverse sol path		
Sol type	*Sol No.*	*Activity*
		Acquire close-approach submillimeter imaging of the drill target (before dust removal)
		Remove dust from the drill target
		Acquire close-approach submillimeter images of the drill target after dust removal
		Dump postsieve (Station D_a) sample
		Acquire context image of postsieve dump site
		Acquire detailed elemental data from the drill spot
Contact	46	Acquire close-approach submillimeter images of postsieve dump pile
		Acquire close-approach submillimeter imaging before drill loading test
		Conduct drill loading test
		Acquire close-approach submillimeter imaging after the drill loading test
		Acquire detailed elemental data from the postsieve dump pile
Contact	47	Using preload data, plan and execute full drill activity (Station D_c)
		Acquire postdrill submillimeter images
Contact/remote	48	Deliver drill sample to high-resolution elemental data analysis
		During the day, collect any desired remote documentation of drill hole/tailings
		Acquire millimeter-scale imaging of drill hole for future reflectance spectroscopy targeting
		First high-resolution data integration of sample
Contact/remote	49	Acquire reflectance spectroscopy data from drill hole interior
		Complete any further daytime remote documentation of the drill hole/tailings
		At night, submillimeter imaging of drill hole interior and tailings
		Acquire detailed elemental data from the drill tailings
Contact/remote	50	Complete drill hole/tailings observations
		Conduct second mineralogical analysis of Station D_c sample

XRD = X-ray Diffractometer.

Supplementary Table S2. Estimated Sol Cost for All Activities by the Walkabout Team

Walkabout traverse sol path		
Sol type	*Sol No.*	*Activity*
Drive/remote	1	Approach Station 1
		Acquire 3 tier (ground to sky) 180° mosaic pointed ~N
Drive	2	Bump to Station 1a reflectance spectroscopy location using image 4457 from the 180° mosaic
Remote/drive	3	Select and acquire three spots for reflectance spectroscopy analysis
Drive/remote	4	Drive to Station 2 using Sol 3 drive direction mosaic
		Acquire new 3 tier 360° mosaic
Drive	5	Bump to Station 2a reflectance spectroscopy location using image 4495 from the 360° mosaic
Drive/remote	6	Acquire one large reflectance spectroscopy raster
		Drive to Station 3 using Sol 4 mosaic
		Acquire new 3 tier 360° mosaic
Drive	7	Bump to Station 3a using Sol 6 mosaic
Drive/remote	8	Select and acquire two reflectance spectroscopy 10×1 rasters of red bed and shaley unit
		Drive to Stop 4 using Sol 6 mosaic
Remote	9	Acquire 3 tier 360° mosaic
Drive/remote	10	Acquire millimeter-scale images of potential close domal structures (interpretation: stromatolites)
		Bump to Station 4a using Sol 9 mosaic
Drive/remote	11	Select and acquire three reflectance spectroscopy 5×1 rasters of domal material
		Bump to Station 4.1 using Sol 6 mosaic
Remote	12	Select and acquire two reflectance spectroscopy 5×1 rasters of light and dark gray domal material
		Millimeter-scale imaging of more distant domal structures
Drive/remote	13	Drive to Station 5 using Sol 9 mosaic
Drive	14	Drive to Station 5 (distance >50–100 m)
		Acquire new 3 tier 360 mosaic
		Acquire two clast survey images

(*continued*)

Supplementary Table S2. (Continued)

Walkabout traverse sol path		
Sol type	*Sol No.*	*Activity*
Drive	15	Bump to Station 5a reflectance spectroscopy location using image 6183 from the 360° mosaic
Remote/drive	16	Select and acquire two 5×1 rasters of lumpy and vertical structures
		Drive to Station 6 using Sol 12 mosaic
Remote	17	Acquire new 3 tier 360 mosaic
		Acquire two clast surveys
		Acquire two 5×1 rasters (faulted out)
Drive	18	Return to Station 2 for the beginning of loop 2 (distance >50–100 m)
Drive	19	Return to Station 2 (distance >50–100 m)
Drive	20	Return to Station 2 (distance >50–100 m)
Contact	21	Acquire millimeter-scale images of surficial textures of beds
		Acquire MAHLI image of odd-textured beds
		Overnight elemental data acquisition on target for submillimeter imaging
Drive	22	Drive to Station 3 (loop 2)
		Acquire 3×2 workspace mosaic
Contact/drill	23	Select spot for sampling on layer with wavy laminations to plan drill placement
		Submillimeter predust removal and preload images
		Dust removal from drill spot
		Submillimeter postdust removal images
		Preload test
		Post-preload test images
		Overnight elemental data acquisition on drill spot
Contact	24	Using preload data, plan and execute full drill activity on Stop 3 sample
		Acquire postdrill submillimeter images
Contact/remote	25	Deliver drill sample to XRD instrument
		During the day, collect any desired remote documentation of drill hole/tailings
		Acquire millimeter-scale imaging of drill hole for future reflectance spectroscopy targeting
		First high-resolution data integration of sample
Contact/remote	26	Acquire reflectance spectroscopy data from drill hole interior
		Complete any further daytime remote documentation of the drill hole/tailings
		At night, submillimeter imaging of drill hole interior and tailings
		Acquire detailed elemental data from the drill tailings
Drive/remote	27	Complete drill hole/tailings observations
		Drive to Station 4.1
		Acquire 3×2 workspace mosaic
Contact/drill	28	Select spot for sampling on layer with wavy laminations to plan drill placement
		Submillimeter predust removal and preload images
		Dust removal from drill spot
		Submillimeter postdust removal images
		Preload test
		Post-preload test images
		Overnight elemental data acquisition on drill spot
Contact	29	Using preload data, plan and execute full drill activity on Stop 4.1
		Acquire postdrill submillimeter images
Contact/remote	30	Deliver drill sample to high-resolution elemental data analysis
		During the day, collect any desired remote documentation of drill hole/tailings
		Acquire millimeter-scale imaging of drill hole for future reflectance spectroscopy targeting
		First high-resolution data integration of sample
Contact/remote	31	Acquire reflectance spectroscopy data from drill hole interior
		Complete any further daytime remote documentation of the drill hole/tailings
		At night, submillimeter imaging of drill hole interior and tailings
		Acquire detailed elemental data from the drill tailings
Drive/remote	32	Complete drill hole/tailings observations
		Drive to Station 5
		Acquire 3×2 workspace mosaic
Contact/drill	33	Select spot for sampling on layer with wavy laminations to plan drill placement
		Submillimeter predust removal and preload images
		Dust removal from drill spot
		Submillimeter postdust removal images
		Preload test
		Post-preload test images
		Overnight elemental data acquisition on drill spot

(*continued*)

Supplementary Table S2. (Continued)

Walkabout traverse sol path		
Sol type	*Sol No.*	*Activity*
Contact	34	Using preload data, plan and execute full drill activity on Stop 5 Acquire postdrill submillimeter images
Contact/remote	35	Deliver drill sample to high-resolution elemental data analysis During the day, collect any desired remote documentation of drill hole/tailings Acquire millimeter-scale imaging of drill hole for future reflectance spectroscopy targeting First high-resolution data integration of sample
Contact/remote	36	Acquire reflectance spectroscopy data from drill hole interior Complete any further daytime remote documentation of the drill hole/tailings At night, submillimeter imaging of drill hole interior and tailings Acquire detailed elemental data from the drill tailings
Drive/remote	37	Complete drill hole/tailings observations

MAHLI = Mars Handlens Imager.